ARTICLE TYPE

The shape of D-glucosamine

Isabel Peña, Lucie Kolesniková, Carlos Cabezas, Celina Bermúdez, Matías Berdakin, Alcides Simão and José L. Alonso*

The bioactive amino monosaccharide D-glucosamine has been generated in gas phase via laser ablation of D-glucosamine hydrochloride. Three cyclic α-$^4C_1$ pyranose forms have been identified using Fourier transform microwave techniques. Stereoelectronic hyperconjugative forces – essentially linked with the anomeric or gauche effect – and cooperative OH···O, OH···N and NH···O chains, extended along the entire molecule, are found to be the main factors driving the conformational behavior. The orientation of the NH_2 group within each conformer has been determined by the values of the nuclear quadrupole constants. The results have been compared with those recently obtained for the archetypical D-glucose.

Introduction

The first conformational characterization of isolated D-glucose molecule in gas phase became recently possible due to the latest developments of Fourier tranform microwave techniques coupled with laser ablation vaporizations methods.[1] For this archetypical monosaccharide, four conformers of α-D-glucopyranose and three of β-D-glucopyranose have been unequivocally identified. D-glucosamine ($C_6H_{13}NO_5$, see Figure 1a) is a bioactive amino monosaccharide that differs structurally from the parent D-glucose by replacement of the hydroxyl group on C_2 by an amino group. In the human body, glucosamine is biochemically formed as glucosamine-6-phosphate,[2] which is an essential precursor for subsequent synthesis of important nitrogen-containing macromolecules, such as glycoproteins, glycolipids and glycosaminoglycans, known as building blocks of the joint cartilage and connective tissues, contributing to their strength and flexibility.[3] Glucosamine salts, derivatives and glucosamine-containing polymers have potential to be used in numerous biomedical applications.[3-7]

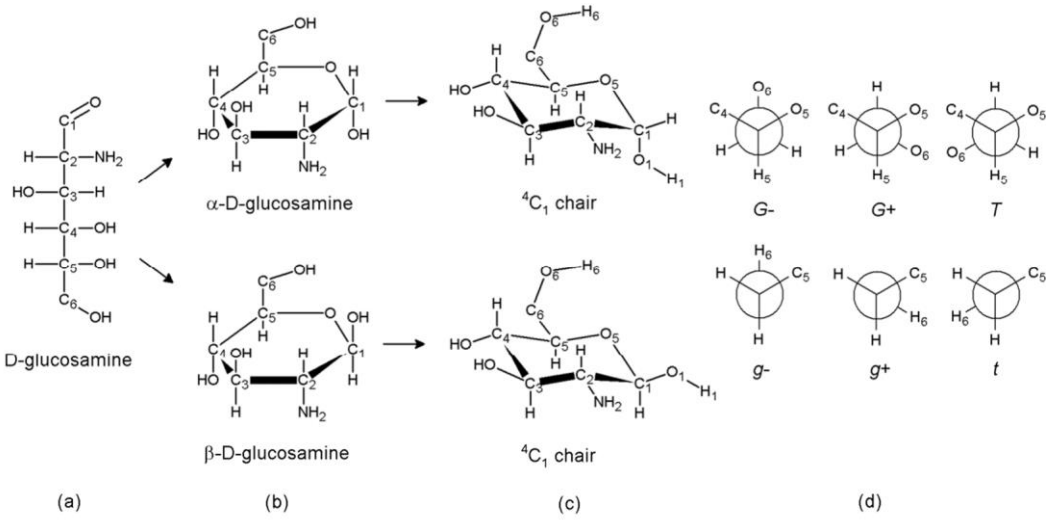

Fig. 1 (a) Fisher projection of D-glucosamine; (b) α- and β-anomers of D-glucosamine in Haworth projection; (c) $^4C_1$ conformations of α- and and β-D-glucosamine; (d) Newman projections of plausible conformations of the hydroxymethyl group around the C_5-C_6 (*G*−, *G*+, *T*) and C_6-O_6 (*g*−, *g*+, *t*) bonds.

In the pure form, D-glucosamine is chemically unstable; promptly reacting when exposed to the atmosphere, and is thus only commercially available as a salt, where it appears in the protonated form. Hence, most of the experimental studies on D-glucosamine salts have been performed in either the solid[8-10] or liquid phases.[10-15] X-ray crystallography experiments on D-glucosamine hydrochloride indicate that the protonated glucosamine exists in the α-anomeric pyranose form, in the preferred $^4C_1$ chair conformation.[8,9] When dissolved in water, the α-pyranose form is slowly transformed into the β-form, until it

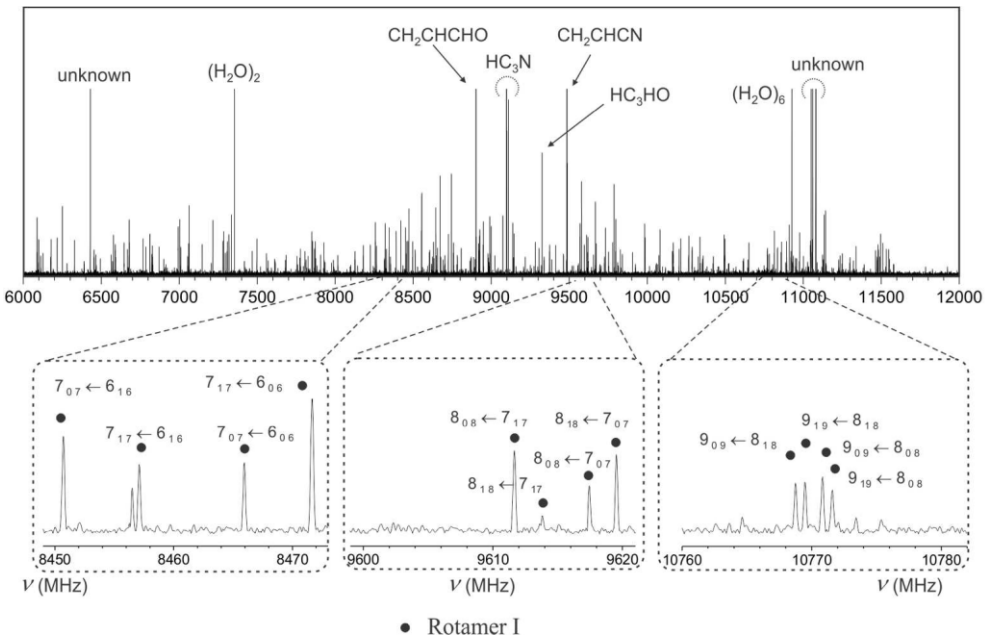

Fig. 2 Upper panel: overview CP-FTMW spectrum of the laser ablated α-D-glucosamine with assigned decomposition lines; lower panels: a-type $(J+1)_{0\,J+1} \leftarrow J_{0\,J}$, $(J+1)_{1\,J+1} \leftarrow J_{1\,J}$ and b-type $(J+1)_{1\,J+1} \leftarrow J_{0\,J}$, $(J+1)_{0\,J+1} \leftarrow J_{1\,J}$ progressions in detail corresponding to the observed rotamer I; rotational transitions become degenerated with the increasing J.

reaches the equilibrium anomeric composition of α: β ~ 63:37 as observed from optical rotation and nuclear magnetic resonance (NMR) experiments.[11,12] Interestingly, these results contrast with those obtained for D-glucose, where the reversed ratio of the two anomeric forms has been reported.[12,14-16] Despite the biological and medical importance of D-glucosamine, no experimental data on the conformational behavior of its neutral form has been reported hitherto.

At the University of Valladolid, efficient procedures have been developed for generation of neutral forms of proteogenic amino acids in supersonic expansion by laser ablation of its zwitterionic forms, allowing their conformational investigation using Fourier transform microwave techniques.[17,18] These experimental approaches have also been applied successfully to many other biologically relevant molecules, and, recently, several conformers of the monosaccharides D-glucose,[1] D-xylose,[19] D-fructose,[20] D-ribose,[21] 2-deoxy-D-ribose[22] and D-erythrose[23] have been identified and characterized structurally. In the present study, the conformational behavior of D-glucosamine, successfully generated in the gas phase by laser ablation of its hydrochloride salt, is reported for the first time.

Experimental

A commercial sample of D-glucosamine hydrochloride (m.p. = 190 – 194 °C) was used without any further purification. A solid rod was prepared by pressing the compound's fine powder mixed with a small amount of commercial binder and was placed into the ablation nozzle. A picosecond Nd:YAG laser (10 mJ per pulse, 35 ps pulse width) was used as vaporization tool. Products of the laser ablation were supersonically expanded using the flow of carrier gas (Ne, 15 bar) into the vacuum chamber of the spectrometers. D-glucosamine was first investigated using a chirped pulse Fourier transform microwave (CP-FTMW) spectrometer coupled with laser ablation to sample swiftly the rotational spectra of the different conformers present in the gas-phase mixture. Details of the experimental setup have been given elsewhere.[17] Up to 70 000 individual free induction decays were averaged in the time domain and Fourier transformed to obtain the rotational spectrum from 6 to 12 GHz shown in the upper panel of Figure 2. A Kaiser-Bessel window was applied to increase the baseline resolution. The sub-Doppler resolution of the laser ablation molecular beam Fourier transform microwave (LA-MB-FTMW) technique,[18] operating from 4 to 18 GHz, was used to resolve the hyperfine structure due to the ^{14}N nucleus. A short microwave radiation pulse of 0.3 μs duration was applied to polarize all the vaporized molecules. The registered free induction decay was then converted to the frequency domain by Fourier transformation. All the transitions appeared as Doppler doublets due to the parallel configuration of the molecular beam and the microwave radiation. The resonance frequency was determined as the arithmetic mean of the two Doppler components. Frequency accuracy better than 5 kHz and an estimated resolution of 7 kHz are achieved in the experiment.

Results

a. Modelling

Similarly to D-glucose and other hexoses, D-glucosamine may exist in linear or cyclic forms, with the six-membered aldopyranose ring being the most stable species[24] (see Figure 1b). The formation of this ring structure is the result of a cyclization process through the nucleophilic attack of the hydroxyl group located at C_5 to the carbonyl carbon atom (C_1), which may lead to formation of α and β anomeric forms. The pyranose ring might assume either of two chair $^1C_4$ or $^4C_1$ configurations (see Figure 1c), but being dominant the latter, where the hydroxymethyl -CH_2OH group is in equatorial position and is energetically

Table 1. Molecular properties for the α- and β- lowest energy conformers of D-glucosamine (below 600 cm^{-1}).

	A[a]	B	C	χ_{aa}	χ_{bb}	χ_{cc}	$\lvert\mu_a\rvert$	$\lvert\mu_b\rvert$	$\lvert\mu_c\rvert$	ΔE^b	ΔG^c
α-G-g+/*cc*/t	1276	784	581	2.21	−3.92	1.70	3.0	3.8	0.1	0	0
α-G+g-/*cc*/t	1313	763	534	0.66	−2.44	1.78	3.0	3.2	1.2	31	19
α-Tg+/*cc*/t	1398	740	538	2.54	−4.33	1.79	4.1	1.7	0.9	113	205
α-G-g+/*cl*/g-	1296	788	573	2.76	0.51	−3.26	1.0	0.7	1.2	329	327
α-Tt/*cl*/g-	1404	752	544	2.76	0.46	−3.22	2.4	0.6	0.3	541	613
α-Tg-/*cl*/g-	1400	748	542	2.75	0.40	−3.15	0.1	0.5	0.0	587	672
β-G-g+/*cc*/t	1177	818	535	2.34	-3.37	1.03	2.8	2.2	2.5	0[d]	0
β-G+g-/*cc*/t	1180	790	495	0.70	-2.38	1.68	2.6	2.0	1.0	37	16
β-Tg+/*cc*/t	1317	735	495	2.40	-4.10	1.71	3.2	0.4	1.0	140	230

[a] A, B, and C represent the rotational constants (in MHz); χ_{aa}, χ_{bb} and χ_{cc} are the diagonal elements of the ^{14}N nuclear quadrupole coupling tensor (in MHz); μ_a, μ_b and μ_c are the electric dipole moment components (in D). [b] Relative energies (in cm^{-1}) with respect to the global minimum calculated at the MP2/6-311++G(d,p) level. [c] Gibbs energies calculated at 298 K. [d] The α-anomer species is predicted to be 579 cm^{-1} more stable than the β-anomer.

favored[1] (see Figure 1c). On this basis, *ab initio* calculations were performed on α- and β- $^4C_1$ configurations to obtain the lower-energy conformations and their relative Gibbs energies. Six α and three β forms have been predicted below 600 cm^{-1} (see Table 1). The α and β glucosamine´s conformers have been labeled according to the hydroxymethyl group configurations.[1,25] Three staggered forms, designated *G*−, *G*+ (*gauche*) and *T* (*trans*) (see Figure 1d), and represented by the $O_6-C_6-C_5-O_5$ dihedral angle with the values of approximately −60°, 60° and 180°, respectively, have been considered. In the same way, the symbols *g*−, *g*+ and *t* describe the conformations defined by the $H_6-O_6-C_6-C_5$ dihedral angle. The symbols *cc* or *cl* after the first slash denote, respectively, the counterclockwise or clockwise arrangement of the cooperative network of intramolecular hydrogen bonds. Finally, after the second slash, the symbols *g*−, *g*+ and *t* represent the orientation of the anomeric hydroxyl group hydrogen atom defined by the $H_1-O_1-C_1-C_2$ dihedral angle.

The Moller-Plesset second order method (MP2) and the 6−311++G(d,p) basis set[26] were used to geometrically optimize the structures and to calculate the relevant spectroscopic properties. The values of the rotational constants (*A*, *B*, *C*), electric dipole moment components (μ_a, μ_b, μ_c) and the electric quadrupole coupling constants (χ_{aa}, χ_{bb}, χ_{cc}) for these conformers are reported in Table 1.

b. Broadband CP-FTMW rotational spectrum analysis

The recorded broadband rotational spectrum of laser ablated of D-glucosamine hydrochloride from 6 to 12 GHz is shown in Figure 2. Soon, decomposition products lines common to other studies of sugars[20a] and amino acids[27] (see Figure 2, upper panel) attributable to cyanoderivatives, formadelhyde, etc. were easily identified. After excluding the aforementioned signals from the spectral analysis, the identification of rotational transitions belonging to a first species, labeled as rotamer I, was accomplished. Assignments were based on the identification in the broadband spectrum of *a*-type $(J+1)_{0\,J+1} \leftarrow J_{0\,J}$, $(J+1)_{1\,J+1} \leftarrow J_{1\,J}$ and *b*-type $(J+1)_{1\,J+1} \leftarrow J_{0\,J}$, $(J+1)_{0\,J+1} \leftarrow J_{1\,J}$ pairs of rotational progressions, which became degenerated with increasing J (Figure 2, lower panels). Following an iterative procedure of fitting and subsequent predictions, more *a*-type and *b*-type transitions were assigned in the range from $J = 3$ to $J = 8$.

On the same basis, further searches in the broadband spectrum made possible the assignment of rotational transitions of another two rotamers: II and III. For rotamer III, only a-type rotational transitions were observed. No other rotamers were found in the broadband rotational spectrum.

Table 2. Experimental spectroscopic parameters for the three observed rotamers of D-glucosamine obtained from CP-FTMW spectra.

Parameter	**Rotamer I**	**Rotamer II**	**Rotamer III**
A[a] / MHz	1269.4108 (23)[e]	1305.3545 (29)	1389.896 (18)
B / MHz	781.1783 (13)	760.1481 (12)	738.65091 (94)
C / MHz	577.43929 (36)	531.25706 (33)	535.50479 (54)
a-type [b]	observed	observed	observed
b-type	observed	observed	–
c-type	–	–	–
N[c]	31	42	21
σ_{fit}[d] / kHz	23.3	26.1	19.2

[a] A, B, and C represent the rotational constants. [b] Observation of a-, b-, and c-type transitions for each structure. [c] Number of fitted transitions. [d] RMS deviation of the fit. [e] Standard error in parenthesis in the units of the last digit.

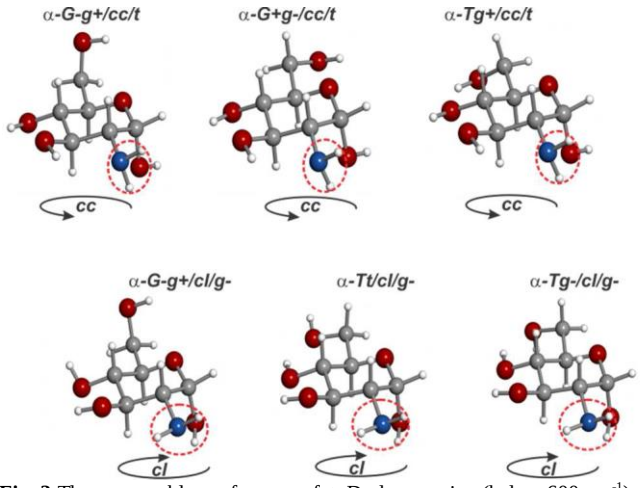

Fig. 3 The most stable conformers of α-D-glucosamine (below 600 cm^{-1}), showing the *cc* configuration in conformers *G-g+/cc/t*, *G+g-/cc/t* and *Tg+/cc/t* and the *cl* one in conformers *G-g+/cl/g-*, *Tt/cl/g-* and *Tg-/cl/g-*.

Some observed transitions show partial resolved hyperfine structure as corresponding to a compound with one ^{14}N nucleus. No transition with a quadrupole hyperfine structure as corresponding to a chlorine nucleus was found. These experimental facts confirmed the generation of neutral glucosamine in the gas phase by laser ablation of crystalline D-glucosamine hydrochloride and the absence of the salt in the supersonic expansion. Thus, the three observed rotamers can be ascribed to different glucosamine conformers. Since the spectral resolution attainable in the CP-FTMW experiments is not sufficient to completely resolve these hyperfine effects, only transitions with unresolved hyperfine structure (see Tables S1-S3 of the ESI†) were fit[28] to a rigid rotor Hamiltonian to derive a first set of the rotational constants listed in Table 2. The comparison of these experimental values with those predicted in Table 1 for the α and β forms of glucosamine clearly indicates that the three observed rotamers belong to α forms of glucosamine shown in Figure 3. The values of the rotational constants reflect directly the mass distribution of the conformers, which is substantially different in α and β forms. Dealing with α forms, it could be hypothesized that rotamer I could be the *G-g+/cc/t* or *G-g+/cl/g-* conformers and rotamer III the *Tg+/cc/t*, *Tt/cl/g-*, or *Tg-/cl/g-* conformers, while rotamer II can be definitively assigned to *G+g-/cc/t* conformer. If two conformers present similar mass distribution, the rotational constants cannot be used to unambiguously distinguish between them. Hence, other conformational tools are needed for a conclusive identification.

The intramolecular hydrogen bond network arrangements, counterclockwise (*cc)* or clockwise (*cl*) (see Figure 3), significantly changes the predicted values of the dipole moment components for the six plausible low-energy conformes of the α forms (see Table 1). It, consequently, affects the observable type of transitions. Table 2 documents that none of *c*-type transition was observed for the various rotamers. If rotamer I was indeed the *G-g+/cl/g-* conformer, *c*-type transitions should be observable, since $\mu_a \approx \mu_c$. Thus, rotamer I could be tentatively assigned to *G-g+/cc/t* conformer. For rotamer III, only *a*-type transitions were observed, so conformer Tg-/*cl*/g- should be excluded due to very low predicted value for this dipole moment component. It is still not possible to distinguish between conformers *Tg+/cc/t* and *Tt/cl/g-*.

A more straightforward way to distinguish unambiguously between conformers is to take into account the values of nuclear quadrupole hyperfine constants that can be extracted from the hyperfine structure of rotational transitions. The nuclear quadrupole coupling constants derived from the analysis are very sensitive to the orientation of the $-NH_2$ group with respect to the principal axes system. As shown in Table 1, the predicted values for the diagonal elements of the quadrupole coupling tensor χ_{aa}, χ_{bb}, χ_{cc} change dramatically going from the *cc* configuration in conformers *G-g+/cc/t* and *Tg+/cc/t* to the *cl* ones in conformers *G-g+/cl/g-* and *Tg-/cl/g-* (see Figure 3), since the $-NH_2$ group shows opposite orientation in both *cc* and *cl* arrangements to participate in the intramolecular hydrogen bond networks. A high resolution rotational study by LA-MB-FTMW spectroscopy is needed to completely resolve the ^{14}N nuclear quadrupole hyperfine structure, and to achieve a conclusive identification of the observed rotamers.

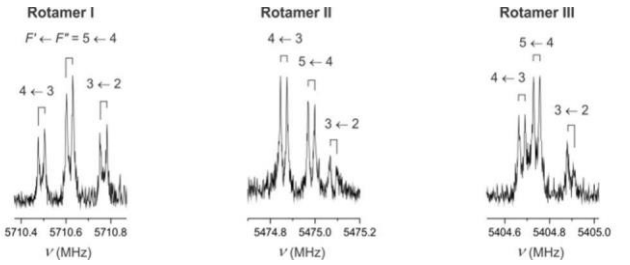

Fig. 4 Nuclear quadrupole hyperfine structure of the $4_{1\,3} \leftarrow 3_{1\,2}$ rotational transition for rotamers I, II and III. Each component labeled as F′←F″ is observed as a doublet due to the Doppler effect. The molecular frequency is the arithmetic mean of the Doppler doublets.

Table 3. Experimental spectroscopic parameters for the three observed rotamers of D-glucosamine obtained from LA-MB-FTMW spectra.

Parameter	**Rotamer I (α-*G-g+/cc/t*)**	**Rotamer II (α-*G+g-/cc/t*)**	**Rotamer III (α-*Tg+/cc/t*)**
A[a] / MHz	1269.4100 (15)[e]	1305.34810 (82)	1390.0011 (14)
B / MHz	781.18234 (26)	760.14999 (14)	738.65282 (13)
C / MHz	577.437380 (86)	531.255624 (50)	535.499914 (56)
χ_{aa}[b] / MHz	2.159 (16)	0.637 (5)	2.487 (6)
χ_{bb} / MHz	−3.727 (14)	−2.278 (4)	−4.129 (5)
χ_{cc} / MHz	1.567 (14)	1.641 (4)	1.642 (5)
N[c]	32	30	18
σ_{fit}[d] / kHz	1.3	1.3	1.1

[a] A, B, and C represent the rotational constants. [b] χ_{aa}, χ_{bb} and χ_{cc} are the diagonal elements of the ^{14}N nuclear quadrupole coupling tensor. [c] Number of fitted transitions. [d] RMS deviation of the fit. [e] Standard error in parenthesis in the units of the last digit

c. High resolution LA-MB-FTMW spectra

A new series of experiments on laser ablated D-glucosamine hydrochloride were carried out using our LA-MB-FTMW technique. The nuclear quadrupole coupling hyperfine structure for the rotational transitions of the observed rotamers was fully resolved as shown in Figure 4 for the 4_{13}-3_{12} transition. A total of 32, 30 and 18 quadrupole hyperfine components were measured for rotamers I, II and III, respectively (Tables S4-S6 of the ESI†). They were analyzed using the effective Hamiltonian $H = H_{ROT} + H_Q$, where H_{ROT} represents the rigid rotor Hamiltonian and H_Q the quadrupole coupling Hamiltonian.[29] Using the $F = J + I$ angular momentum coupling scheme, the energy levels involved in each transition were thus labeled with the quantum numbers J, K_{-1}, K_{+1}, and F. Experimentally derived rotational constants *A*, *B*, *C* together with the diagonal elements of the quadrupole coupling tensor χ_{aa}, χ_{bb}, χ_{cc} for each rotamer are given in Table 3. Contributions of the off-diagonal elements of the nuclear quadrupole coupling tensor to the observed frequencies were found to be negligible, and therefore these parameters were not determined.

At first, a comparison of the experimentally obtained values of the electric quadrupole coupling constants for rotamer II (see Table 3) with the predicted ones (see Table 1) was made to confirm its assignment to the *G+g-/cc/t* conformer. The excellent agreement among both sets of data confirms the assignment based on the rotational constants. Similarly, the experimental electric quadrupole coupling constants for rotamers I and III were

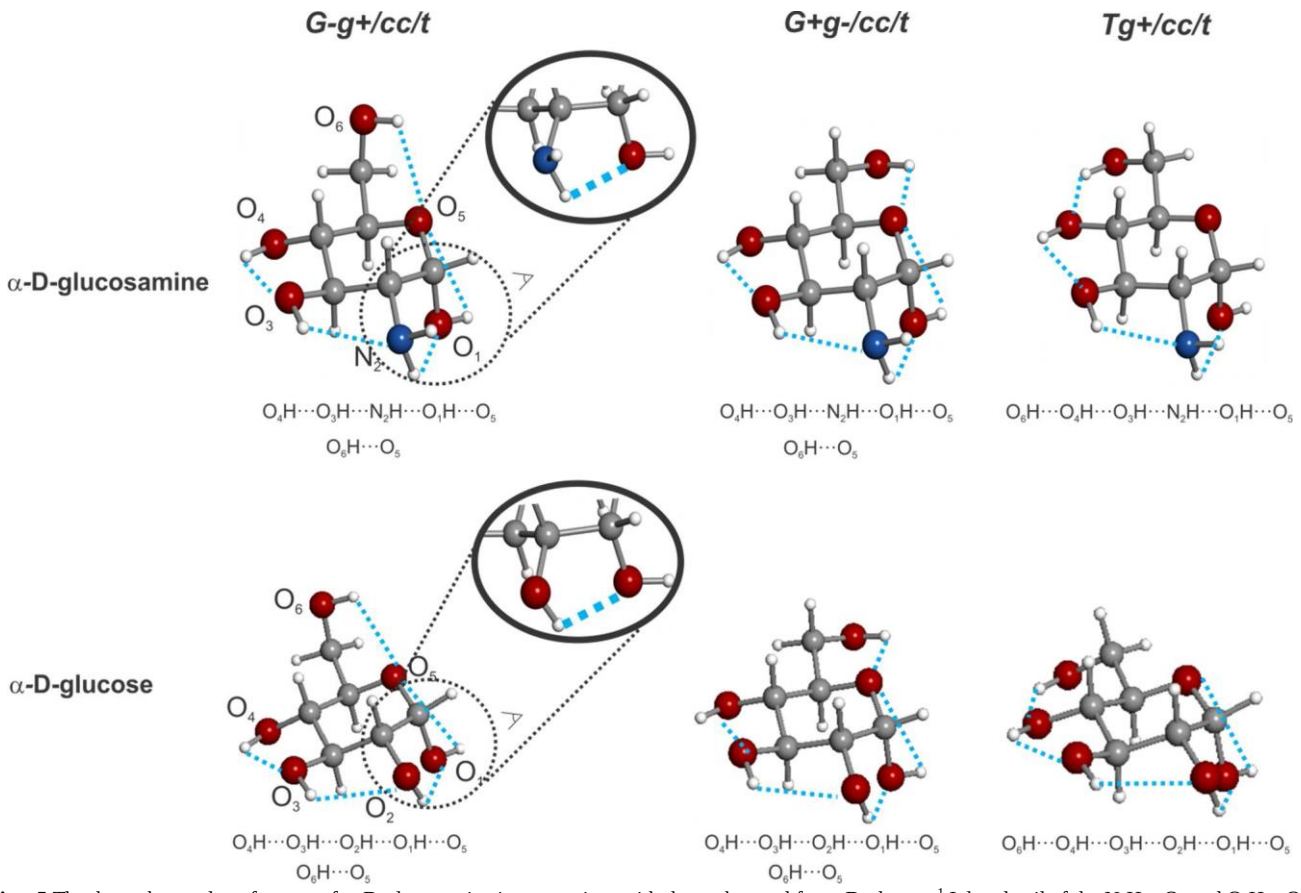

Figg. 5 The three observed conformers of α-D-glucosamine in comparison with those observed for α-D-glucose.[1] Inlet: detail of the $N_2H\cdots O_1$ and $O_2H\cdots O_1$ hydrogen bonds for G-g+/*cc*/t conformers of α-D-glucosamine and α-D-glucose, respectively. The amino group NH_2 in α-D-glucosamine assumes the same role in the intramolecular hydrogen bonding than the hydroxyl group OH in α-D-glucose.

compared with those predicted for the related conformers' candidates (see Tables 3 and 1), unambiguously showing that rotamer I corresponds to the *G-g+/cc/t* conformer and rotamer III corresponds to the *Tg+/cc/t* conformer.

Discussion

The observation of only α-forms deserves some explanation. It should be noted that, as observed in previous studies,[30,31] the laser ablation of solid samples of the crystalline D-glucosamine hydrochloride generates into the gas phase neutral D-glucosamine in its α-pyranose form, thus preserving the α-pyranose species present in the X-ray studies.[1,19] The interconversion between the α and β anomers is a solvent-mediated reaction and thus should not occur that easily during evaporation,[32] especially if the sample is completely dry.[33] In any case, the most stable β form, β-G-g+/*cc*/t, is predicted 579 cm^{-1} above the most stable α-G-g+/*cc*/t one.

The three observed α-pyranose forms of D-glucosamine, G-g+/*cc*/t, G+g-/*cc*/t and Tg+/*cc*/t, are stabilized by the *endo* anomeric effect; they present a $^4C_1$ ring configuration, thus leading the anomeric OH group towards the axial position.[34] The hydroxyl groups are located at the same side of the ring to form a hydrogen bond network, which in turn, is reinforced by sigma hydrogen-bond cooperativity.[35] In this way, the two most stable conformers G+g-/*cc*/t and G-g+/*cc*/t are stabilized by a chain of four cooperative hydrogen bonds ($O_4H\cdots O_3H\cdots N_2H\cdots O_1H\cdots O_5$) and one non-cooperative $O_6H\cdots O_5$ bond, as depicted in Figure 5. The least stable conformer *Tg+/cc/t* exhibits five cooperative hydrogen bonds ($O_6H\cdots O_4H\cdots O_3H\cdots N_2H\cdots O_1H\cdots O_5$), including the stronger H-bond between O_6H and O_4H which is, for sugars with O_4H equatorial group, favorable only in the *trans* configuration. Relative abundances of the three conformers have been estimated from the relative intensities of the rotational transitions, and found to be G-g+/*cc*/t : G+g-/*cc*/t : Tg+/*cc*/t ≈ 0.7(1) : 1 : 0.2(1), in qualitatively agreement with those predicted for Gibbs energies in Table 1.

The observation of a *trans* configuration for α-D-glucosamine, *Tg+/cc/t*, represents a remarkable fact, since numerous experimental studies on glucopyranosides in condensed phases,[36-38] have shown that the dihedral angle (O6–C6–C5–O5) displays a preference towards G- and G+ gauche configuration, with an almost complete absence of the *trans* (T). Our results are in agreement with *ab initio* computations, which predict the *trans* conformer enough populated to be detected in the supersonic expansion. In any case, the hydroxymethyl group's gauche (G) configurations of D-glucosamine also dominate in the gas phase, which can in principle be seen as a consequence of contributions of factors like the so-called gauche effect,[39] associated with the stabilization of the synclinal (gauche) conformation of two

vicinal electronegative groups bonded to a two carbon unit. The same conformational behavior has been observed in the archetypical α-D-glucopyranose.

As shown in Figure 5, the three observed conformers of α-D-glucosamine and the three lower-energy conformers of α-D-glucose[1] exhibit the same configuration of the exocyclic hydroxymethyl group, as well as the same orientation of the intramolecular hydrogen bond network (*cc*). Their relative abundances are also comparable with those previously reported for the corresponding conformers of α-D-glucose.[1] The fourth conformer in order of increasing energy (*G-g+/cl/g-*) of α-D-glucosamine has not been detected, in contrast to that observed for α-D-glucose. This fact can be easily explained by its higher relative energy and, consequently, to its small abundance in the supersonic expansion.

The high resolution reached by LA-MB-FTMW experiments allows the determination of the nuclear quadrupole coupling constants, χ_{aa}, χ_{bb}, χ_{cc}. They inform on the orientation of the NH_2 group with respect to the molecular frame, and allow establishing the intramolecular interactions in which this functional group is involved. The inlet of Figure 5 shows how the amino group inserts into the hydrogen bond network; it adopts such as orientation to assume the same role of the OH- group at the C_2 carbon in α-D-glucopyranose. Therefore, the amino group does not introduce any changes into the gas phase conformational shape of α-D-glucosamine respect to that observed for α-D-glucose.

Conclusions

The present study provides the first experimental investigation of the gas phase structures of D-glucosamine, which has led to the determination of the conformational behavior of this important amino monosaccharide. Three different conformers have been conclusively identified through their rotational spectra. As with α-D-glucopyranose, the observed conformers are stabilized by a mesh of stereoelectronic hyperconjugative forces – essentially linked with the anomeric or *gauche* effect – and cooperative OH···O chains extended along the entire molecule. The three observed conformers of α-D-glucosamine and the three most abundant conformers of α-D-glucose have the same configurations of the hydroxymethyl group as well as the same counterclockwise arrangement of the OH groups. The orientation of the NH_2 group within each conformer has been delineated by the values of the nuclear quadrupole constants. The NH_2 group adopts the same role than the OH group in the intramolecular hydrogen bonding network, which leads to the conclusion that the substitution of the hydroxyl group on C-2 by the amino group does not affect the gas phase conformational behavior found in the archetypal D-glucose.

Acknowledgements

This work has been supported by the Ministerio de Ciencia e Innovación (Grants CTQ2010-19008 and Consolider-Ingenio 2010 CSD2009-00038) and Junta de Castilla y León (Grant VA175U13).

Notes and references

Grupo de Espectroscopía Molecular (GEM), Unidad Asociada CSIC, Edificio Quifima, Laboratorios de Espectroscopia y Bioespectroscopia, Parque Científico UVa, Universidad de Valladolid, 47011 Valladolid, Spain. E-mail: jlalonso@qf.uva.es; Fax: +34 983186349; Tel: +34 9831866348

1 J. L. Alonso, M. A. Lozoya, I. Peña, J. C.López, C. Cabezas, S. Mata, S. Blanco, *Chem. Sci.*, 2014, **5**, 515.
2 S. Ghosh, H. J. Blumenthal, E. Davidson, S. Roseman, *J. Biol. Chem.*, 1960, **235**, 1265.
3 G. S. Kelly, *Altern. Med. Rev.*, 1998, **3**, 27.
4 Y. Henrotin, A. Mobasheri, M. Marty, *Arthritis Research & Therapy*, 2012, **14**, 201.
5 T. H. Fischer, A. P. Bode, M. Demcheva, J. N. Vournakis, *J. Biomed. Mater. Res. A*, 2007, **80A**, 167.
6 H. Nakamura, K. Masuko, K. Yudoh, T. Kato, T Kamada, T. Kawahara, *International Journal of Rheumatology*, 2007, **27**, 213.
7 S. X. Wang, S. Laverty, M. Dumitriu, A. Plaas, M. D. Grynpas, *Arthritis & Rheumatism*, 2007, **56**, 1537.
8 Shirley S. C. Chu, G. A. Jeffrey, *Proc. R. Soc. Lond. A.*, 1965, **285**, 470.
9 W. T. A. Harrison, H. S. Yathirajan, B. Narayana, T. V. Sreevidya, B. K. Sarojini, *Acta Cryst.*, 2007, E**63**, o3248.
10 S. C. Sahoo, A. Tharalekshmy, S. W. Ng, P. Naumov, *Crystal Growth & Design*, 2012, **12**, 5148.
11 S. Bunel, C. Ibarra, E. Moraga, A. Blaskó, C. A. Bunton, *Carbohyd. Res.*, 1993, **244**, 1.
12 D. Horton, J. S. Jewell, K. D. Philips, *J. Org. Chem.*, 1966, **31**, 4022.
13 J. C. Irvine, J. C. Earl, *J. Chem. Soc.Trans.*, 1922, **121**, 2370.
14 A. Neuberger, A. P. Fletcher, *Carbohyd. Res.*,1971, **17**, 79.
15 A. Neuberger, A. P. Fletcher, *J. Chem. Soc. B: Phys. Org.*, 1969, 178.
16 T. Taga, K. Osaki, *Bull. Chem. Soc. Jpn.*, 1975, **48**, 3250.
17 S. Mata, I. Peña, C. Cabezas, J. C. López, J. L. Alonso, *J. Mol. Spectrosc.*, 2012, **280**, 91.
18 I. Peña, M. E. Sanz, J. C. López, J. L. Alonso, *J. Am. Chem. Soc.*, 2012, **134**, 2305-2312.
19 I. Peña, S. Mata, A. Martin, C. Cabezas, A. M. Daly, J. L. Alonso, *Phys. Chem. Chem. Phys.*, 2013, **15**, 18243.
20 (*a*) C. Bermúdez, I. Peña, C. Cabezas, A. M. Daly, J. L. Alonso, *ChemPhysChem*, 2013, **14**, 893; (*b*) E. J. Cocinero, A. Lesarri, P. Écija, A. Cimas, B. J. Davis, F. J. Basterretxea, J. A. Fernández, F. Castaño, *J. Am. Chem. Soc*. 2013, **135**, 2845
21 E. J. Cocinero, A. Lesarri, P. Écija, F. J. Basterretxea, J.-U. Grabow, J. A. Fernández, F. Castaño, *Angew. Chem. Int. Ed.* 2012, **51**, 3119.
22 I. Peña, E. J. Cocinero, C. Cabezas, A. Lesarri, S. Mata, P. Écija, A. M. Daly, Á. Cimas, C. Bermúdez, F. J. Basterretxea, S. Blanco, J. A. Fernández, J. C. López, F. Castaño, J. L. Alonso, *Angew. Chem. Int. Ed.*, 2013, **52**, 11840.
23 C. Cabezas, I. Peña, A. M. Daly, J. L. Alonso, *Chem. Commun.*, 2013, **49**, 10826.
24 A. L. Lehninger, *Principles of Biochemistry*; 4th ed.; W.H. Freeman, 2004.
25 M. Hoffmann, J. Rychlewski, *J. Am. Chem. Soc*., 2001, **123**, 2308.
26 M. J. Frisch, G. W. Trucks, H. B. Schlegel, G. E. Scuseria, M. A. Robb, J. R. Cheeseman, G. Scalmani, V. Barone, B. Mennucci, G. A. Petersson, H. Nakatsuji, M. Caricato, X. Li, H. P. Hratchian, A. F. Izmaylov, J. Bloino, G. Zheng, J. L. Sonnenberg, M. Hada, M. Ehara, K. Toyota, R. Fukuda, J. Hasegawa, M. Ishida, T. Nakajima, Y. Honda, O. Kitao, H. Nakai, T. Vreven, J. A. Montgomery Jr., J. E. Peralta, F. Ogliaro, M. Bearpark, J. J. Heyd, E. Brothers, K. N. Kudin, V. N. Staroverov, R. Kobayashi, J. Normand, K. Raghavachari, A. Rendell, J. C. Burant, S. S. Iyengar, J. Tomasi, M. Cossi, N. Rega, J. M. Millam, M. Klene, J. E. Knox, J. B. Cross, V. Bakken, C. Adamo, J. Jaramillo, R. Gomperts, R. E. Stratmann, O. Yazyev, A. J. Austin, R. Cammi, C. Pomelli, J. W. Ochterski, R. L. Martin, K. Morokuma, V. G. Zakrzewski, G. A. Voth, P. Salvador, J. J. Dannenberg, S. Dapprich, A. D. Daniels, O¨. Farkas, J. B.

Foresman, J. V. Ortiz, J. Cioslowski and D. J. Fox, Gaussian 09, Revision B.01, Gaussian, Inc., Wallingford, CT, 2009.
27 M. E. Sanz, C. Cabezas, S. Mata, J. L. Alonso, *J. Chem. Phys.*, 2014, **140**, 204308.
28 H. M. Pickett, J. Mol. Spectrosc., 1991, **148**, 371–377.
29 W. Gordy and R. L. Cook, Microwave Molecular Spectra, John Wiley & Sons, New York, 3rd edn, 1984.
30 C. Cabezas, I. Peña, J. C. López, J. L. Alonso, *J. Phys. Chem. Lett.*, 2013, **4**, 486.
31 C. Cabezas, M. Varela, I. Peña, J. C. López, J. L. Alonso, *Phys. Chem. Chem. Phys.*, 2012, **14**, 13618.
32 P. Finch, *Carbohydrates: Structures, Syntheses and Dynamics*, Kluwer Academic Publishers, Netherlands, 1999.
33 L. P. Guler, Y.-Q. Yu, H. I. Kenttämaa, *J. Phys. Chem. A*, 2002, **106**, 6754 – 6764.
34 E. Juaristi and G. Cuevas, Tetrahedron, 1992, **48**, 5019–5087.
35 G. A. Jeffrey, W. Saenger, *Hydrogen Bonding in Biological Structures*, Springer, New York, 1991.
36 R. H. Marchessault, S. Pérez, *Biopolymers*, 1979, **18**, 2369.
37 K. Bock, J. Ø. Duus, *J. Carbohydr. Chem.*, 1994, **13**, 513.
38 Y. Nishida, H. Hori, H. Ohrui, H. Meguro, *J. Carbohydr. Chem.*, 1988, **7**, 239.
39 S. Wolfe, Acc. Chem. Res., 1972, **5**, 102.